Muthanna Journal of Engineering and Technology, Vol. (12), Issue (1), Year (2024)

Muthanna Journal of Engineering and Technology

Website: https://muthjet.mu.edu.iq/

Submitted 4 December 2023, Accepted 19 December 2023, Published online 6 January 2024

A review of microstructure, residual stresses, and mechanical performance for the welding spot of the alloy steel

Muhaed Alali[a], Raghda Hamdan Jiyad[b]* and S.M. Thahab[c]

[a]*Materials Engineering Department, Faculty of Engineering, University of Kufa, Iraq*
[b]*Materials Engineering Department, Faculty of Engineering, University of Kufa, Iraq*
[c]*Nanotechnology and Advanced Material Research Unit, Faculty of Engineering, University of Kufa, Iraq*
**Corresponding author E-mail: raghda.hamdan.jiad@gmail.com.*

DOI:10.52113/3/eng/mjet/2024-12-01/01-12

Abstract

Spot welding joins various steel types across diverse applications. Notably, it plays a crucial role in automotive manufacturing, where over 5000 spot welds contribute to the structural integrity of each car. This complex process relies on heat and pressure to create "nuggets" of melted metal that bond the sheets together. However, the rapid heating and cooling involved induce significant changes in the material's microstructure, mechanical properties, and residual stresses. These stresses arise from non-uniform expansion and contraction during welding, as well as from phase transformations due to localized heating and cooling. This study delves into these microstructural changes, residual stresses, and mechanical behaviors of spot welds. Additionally, it investigates how welding parameters like current, time, and force influence the joint's strength and residual stresses.

Keywords: *Resistance Spot Welding, Microstructure, Residual stresses, Alloy steel*

1. Introduction

The intricate process of welding utilizes intense heat to fuse multiple metal pieces, ultimately shaping a singular product [1]. Welding creates a strong joint that is more secure than other ways to attach metals. Localized heat production from a heat source occurs during the welding process. The welded pieces were heated up fast to their melt point and then cooled down quickly, which altered the microstructure and mechanical properties and caused residual stresses [2]. Remaining stresses and distortion are two of the most problematic aspects of any welding operation [3]. Uneven heat distribution during resistance spot welding (RSW) creates residual stresses in welded parts due to the differing rates of expansion and contraction in the base metal and the weld. Additionally, rapid heating and cooling combined with phase transformations during cooling contribute to these stresses [4, 5]. As a result, welding introduces complex residual stresses that act as an artificial physiochemical change [6, 7]. Two key factors, weld nugget size and residual stresses, have the most significant impact on the mechanical behavior of the RSW joint. Therefore, it is crucial to understand how RSW parameters affect both of these factors. Notably, welding current has a greater influence than welding time [8]. Both the electric current and welding duration increase residual stresses [9]. In low alloy steel (LAS) welds, the microstructure plays a crucial role in determining the properties of the weld metal. The chemical composition and parameters of the RSW significantly influence the microstructure of the welds. The primary constituent of the LAS weld region's microstructure is acicular ferrite, which ensures weldability and satisfactory mechanical properties of the weld metal [10].

2. Resistance spot welding

2.1. Resistance spot welding fundamentals

Due to its high efficiency and speed, Resistance Spot Welding (RSW) is a crucial joining process in the automotive industries. This method utilizes pressure and high current to join sheet metal parts, as detailed in Figure 1 [11], [12]. By controlling the air pressure in a pneumatic cylinder, the force of the welding can be adjusted. After the workpieces are pressed together for a predetermined amount of time, the power source is connected to a secondary electrical power supply circuit, which includes a welding capacitor, system machine arms, electrodes, and the workpieces themselves [13]. The expansion of the weld nugget is regulated through the management of key parameters, including current, electrode force, and welding duration. Additional variables that impact the formation of welds are electrode distortion, properties of the materials involved, and the presence of gaps between the sheets being joined [14].

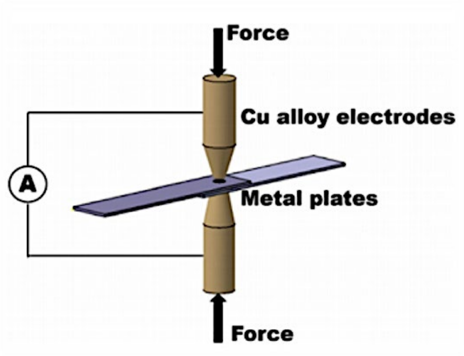

Fig. 1: The schematic representation of the machine of resistance spot welds [15].

The automotive sector is a significant industry that heavily utilizes spot welds to join metal components. A standard automobile body comprises approximately 3000-4000 spot weld joints [16]. The spot-welding process can be executed through manual or robotic means or with a specialized machine tailored for this purpose. Spot welding generates heat according to Joule's law, which is influenced by three factors: the current, the resistance of the conductor, and the duration of the current. The formula for calculating the amount of heat generated can be derived:

$$Q = I^2Rt \tag{1}$$

The formula for calculating heat input (Q) in joules involves the variables of current (I) measured in amperes, resistance (R) measured in ohms, and time (t) measured in seconds. Thus, the quantity of thermal energy produced is contingent upon the aforementioned triad of factors, namely the magnitude of the electrical current, the degree of resistance encountered, and the extent of the welding current's length. [17].

2.2. Resistance spot welding parameters

Welding parameters substantially influence spot welds' characteristics. These variables regulate the weld nugget's microstructure and size, which affects how the welds behave mechanically [18, 19]. These parameters are:

2.2.1. Welding current

Welding current is the most influential parameter in determining the welding performance of a specific material configuration. Increasing of welding current increases the weld nugget diameter and weld strength as shown in Figure 2a and Figure 3a respectively. However, the high welding current causes high temperatures above the melting temperature and leads to an explosion phenomenon in the weld nugget. The expulsion reduces the size of the nugget and could also damage the surrounding machinery and components, the likelihood of porosity in the completed weld increases if the boiling point is reached. Also, excessive electric currents can result in the manifestation of oversized grooves on the metallic surface. Furthermore, the level of heat input directly influences the magnitude of the heat-affected zone (HAZ) and the deformation of the underlying material. It is worth noting that the welding current amplitude typically ranges between 5 and 10 kA, contingent upon the configuration of the sheets [20].

2.2.2. Welding time

Welding time refers to the duration of applying the weld current on the metal plates. All timing functions, including the weld duration, are measured and altered in line voltage cycles. In a power system operating at 50 Hz, one cycle equals 1/50 of a second. It is challenging to determine the ideal weld duration because somewhat dependent on the amount of time needed for the weld spot [21, 22]. The effect of welding time on the nugget diameter and tensile shear strength is shown in Figure 2b and Figure 3b.

2.2.3. Electrode force

The electrodes are fastened to the workpiece to ensure contact between them and the sheets throughout the entire welding process. The electrodes force's function to squeeze metal plates together to form a single unit; otherwise, the weld equality will not be good enough. However, the amount of heat energy will drop as the electrode's force is raised. Therefore, a high weld current is needed to produce the same electrode force. A spatter will form between the electrode and the sheet and the electrode will become caught in the sheet [23]. Figures 2c and 3c highlight the fact that the force applied to the electrode can have a variable effect on both the size and strength of the welded area.

2.2.4. Squeeze time

The Squeeze Time is the amount of time that passes between when an electrode initially touches a piece of work and when current is applied. Squeeze times are required to delay the electrode's end when the electrode's force reaches the desired level [21].

2.2.5. Holding time

Once the welding process is complete, the current is switched off. However, the electrodes remain attached to the welded metal sheets to allow them to cool down. This period, known as the hold time, is crucial for the solidification of the weld nugget and ensures proper cooling of the welded area [24].

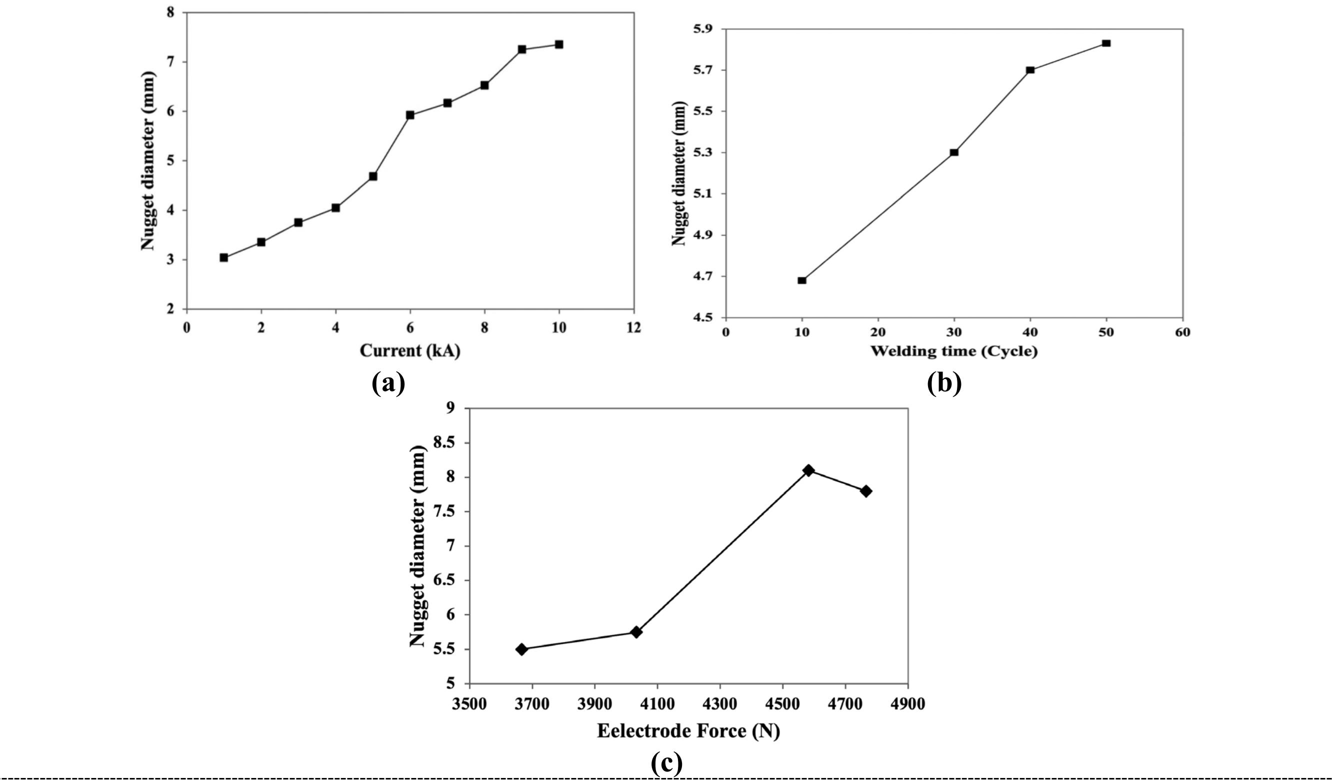

Fig. 2: Effect of (a) welding current, (b) welding time, and (c) electrode force on nugget diameter. Adapted from [25, 26]

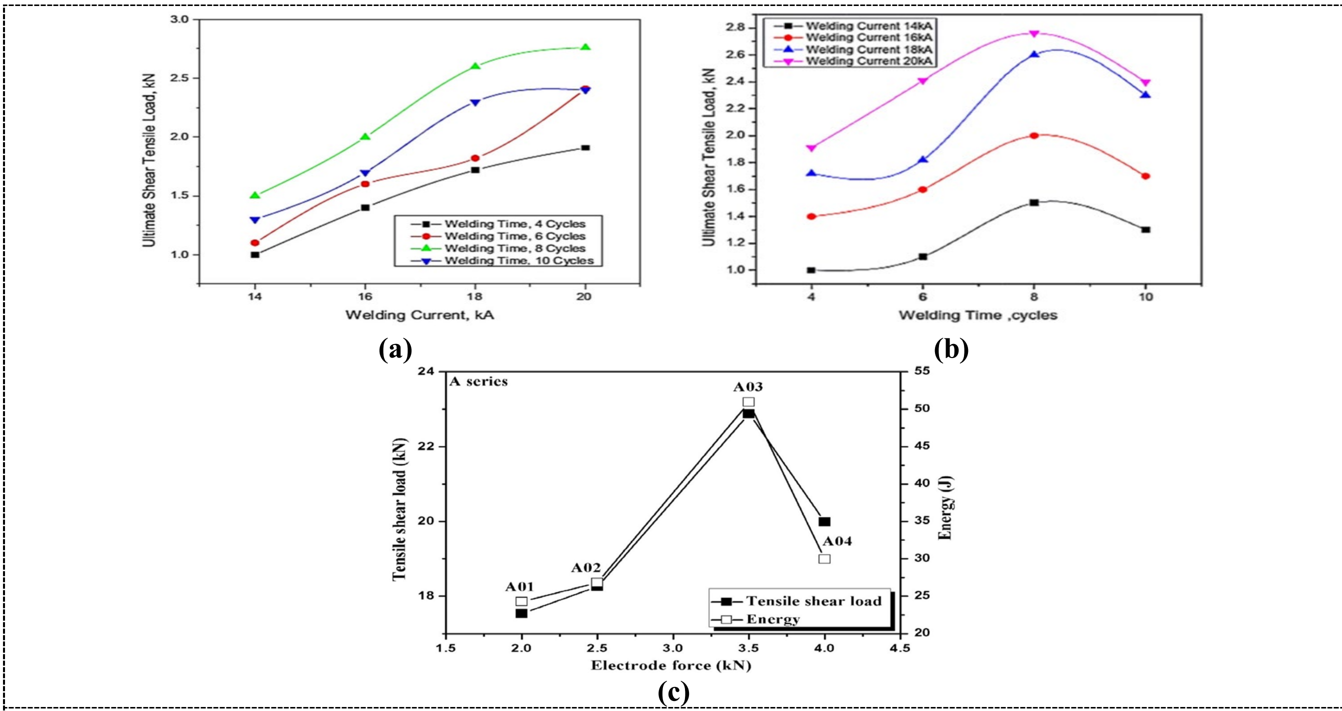

Fig. 3: Effect of (a) welding current, (b) weld time, and (c) electrode force, on tensile shear load. Adapted from [27, 28]

3. Microstructure in spot welded alloy steel

The microstructure of an alloy steel spot weld can be separated into a BM, fusion zone (FZ), HAZ, and partially melted zone (PMZ) as illustrated in Figure 4a [29]. BM is the zone that is unaffected during the welding, and the microstructure remains the same. The microstructure, as depicted in Figure 4(b), was characterized by a ferrite matrix containing carbides that were dispersed along the grain boundaries [30]. The FZ experiences the highest temperature, leading to typical recrystallization. The microstructure observed in Figure 4c reveals the presence of coarse lath martensite in the fusion zone due to fast cooling. During the process of welding, the liquid metal initially undergoes a common phenomenon known as twinning crystallization at the semi-melted grains. Austenite undergoes precipitation along the fusion line, exhibiting growth in the direction of the electrode's action, and ceases growth upon reaching the center. The formation of columnar martensite occurs through the process of water cooling within the electrode [29], resulting in a distinct directional pattern. The growth orientation is roughly aligned with the direction of the electrode, specifically along the direction of the temperature gradient. In this particular region, the dendrites undergo a process of solid-solid transformation after the solidification stage. The columnar grains are composed of characteristic martensite laths [31]. The HAZ is divided into three regions inter-critical heat affected zone (ICHAZ), fine grain heat affected zone (FGHAZ), and coarse grain heat affected zone (CGHAZ). The microstructure of ICHAZ in Figure 4d is composed of lath martensite and ferrite. Austenite changes to fine lath martensitic after cooling in water [29]. The FGHAZ is located between the inner layer adjacent to the (CGHAZ), and the outer layer (ICHAZ), Figures 4 (e) and (f) illustrate the customary microstructures of the FGHAZ and CGHAZ, respectively. Is fine martensite and prior austenite grain (PAG) boundaries. The length of the martensite lathes in the (FGHAZ) is comparatively shorter than that in the (CGHAZ), potentially due to the constraint imposed by the smaller size of the prior austenite grains (PAG) in the FGHAZ [32]. When PMZ is heated to a temperature between solidus and liquidus in Figure 4g, a variety of materials partially melt [33]. The phase transformation of HAZ is induced by thermal cycling and the application of electrode pressure. In the welding procedure, both the CGHAZ and FGHAZ undergo complete austenitization. The CGHAZ, in particular, experiences prolonged exposure to high temperatures, resulting in its microstructure being fully austenitized. This austenitized microstructure closely resembles that of the nugget zone. They are facilitating the dispersion of carbon and the development of austenite. Following the process of water cooling, a significant quantity of coarse lath martensite is generated [31].

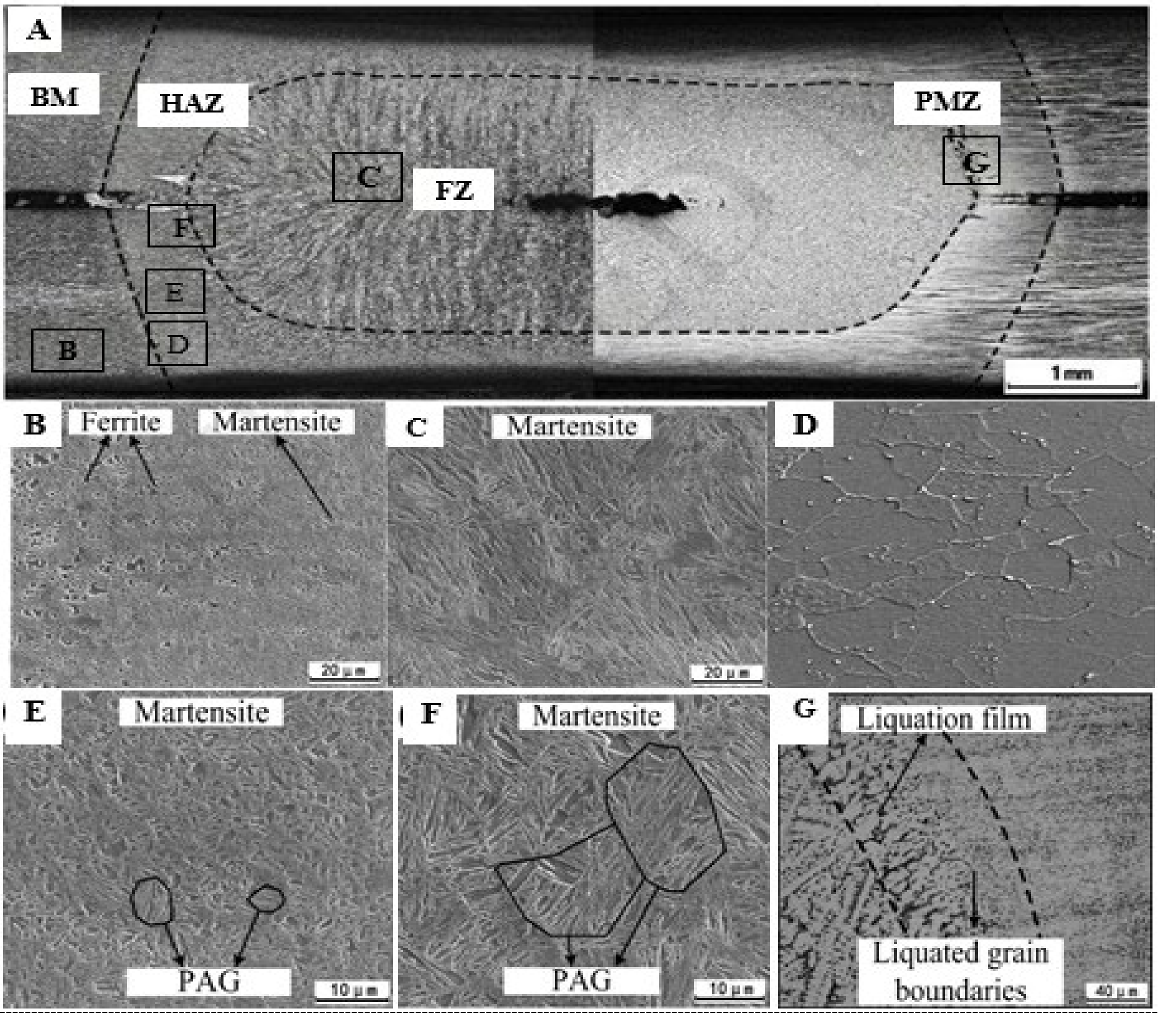

Fig. 4: Microstructure evolution at resistance spot welding : (A) A general view of the etched sample, (B) base metal, (C) fusion zone, (D) inter-critical HAZ, (E) fine grain HAZ, (F) coarse grain HAZ, (G) partially melted zone (PMZ).

4. Mechanical properties of spot welded joint

4.1. Tensile properties

The strength and reliability of the spot welds, as well as the overall construction of the car, play crucial roles in determining its crashworthiness [35]. The welds are examined under the tensile shear test, which uses a typical tensile testing machine apparatus [36]. Higher welding current leads to larger nuggets, which in turn translates to a higher maximum load capacity before fracture. However, there were fluctuations observed in the ultimate load capacity for fracture, as well as the failure energy, with varying levels of welding current [37]. In a 2002 study, Al-Mukhtar investigated the spot welding of austenitic stainless steel (321). He explored the influence of various welding parameters on the mechanical properties of the welded joints. His findings revealed a direct relationship between the strength and area of the weld joint, and the variables of welding current, time, and electrode tip diameter. Increasing these parameters resulted in a corresponding increase in both weld joint strength and area [38]. A 2006 study by S. Aslanlar explored how welding parameters influence the strength of resistance spot welds in chromite micro-alloy steel sheets. They focused on the effects of welding current, welding time, and nugget size on both tensile-peel and shear strength. Their findings revealed a direct relationship between welding parameters and nugget diameter, with larger nuggets resulting from higher currents and longer welding times. Notably, the maximum tensile-peel strength coincided with the largest nugget size, which also translated to increased tensile shear strength [39]. Pouranvari et al. (2010) investigated how welding current, time, force, and holding time affect the strength and size of spot welds in low-carbon steel. Increasing current and time improved strength and size, while higher force weakened the welds and made them smaller [40]. Pouranvari (2011) studied the effect of welding current on the strength of spot welds made in low-carbon steel sheets under tensile-shear loading. They found that increasing the welding current increases both the maximum force the weld can handle (peak load) and the amount of energy it can absorb before failing (failure energy). This is because a higher current leads to a larger molten zone (fusion zone) and deeper penetration of the weld [41]. The impact of the welding current on the dimensions of the nugget and the maximum load is depicted in Figure 5.

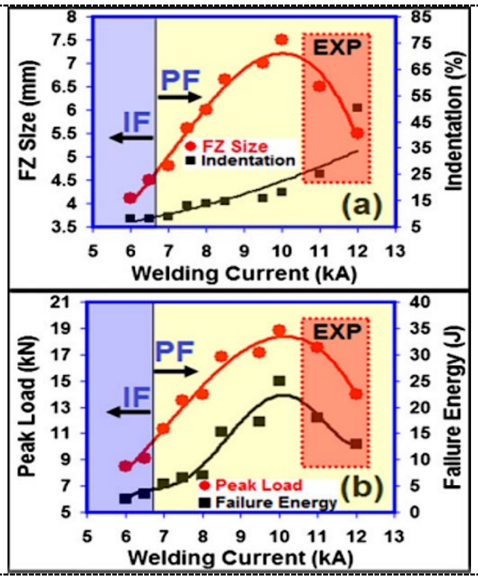

Fig. 5: The impact of welding current on a) the size of the fusion zone and the depth of electrode indentation, and b) the maximum load and energy required for failure. Adapted from [42].

4.1.1. Mechanism and mode failure in the tensile strength loading state

The analysis of weld fracture surfaces aims to identify spot weld failure modes under various welding conditions. Two primary failure modes, namely interfacial failure (IF) and pullout failure (PF), were observed in both tensile-shear and cross-tension tests. The size of the fusion zone (FZ) is widely recognized as the key physical attribute influencing the mechanical characteristics and failure modes of resistance spot welds (RSWs) [43]. In the IF mode, a crack propagates through the fusion zone, while the PF mode involves extracting the nugget from one of the sheets, leading to failure. The mode of failure significantly impacts the carrying capacity and energy absorption capacity of RSWs. In cases of IF mode failure, crucial for the crashworthiness of vehicles in automotive design, there may be a substantial compromise. Failures of interfacial welds under low loads affect load distribution. To prevent PF mode failure, adjustments to welding conditions are necessary, as failure to do so may result in buckling and a reduction in the structural components' ability to absorb crushing energy [44]. The IF mode is primarily influenced by shear stress, whereas the PF mode is driven by tensile stress along the nugget's perimeter [45].

4.2. Microhardness

One crucial aspect influencing the investigation of resistance spot welds' failure mechanisms is their hardness attribute [43]. The magnitude of the fusion zone plays a pivotal role in influencing mechanical properties, particularly microhardness. A Vickers hardness testing device is utilized to evaluate the microhardness characteristics of spot welds. The hardness assessments are conducted in the fusion zone (FZ), heat-affected zone (HAZ), and base metal (BM) throughout the weldment [46]. This examination involves both longitudinal and transverse analyses of microhardness, as illustrated in Figure 6 and Figure 7. These figures depict investigations across the flaying surface and thickness, respectively [47].
Compared to the base metal (BM) and heat-affected zone (HAZ), the microhardness of the nugget zone demonstrates a substantial increase, registering hardness levels ranging from 350 Hv to 450 Hv. Specifically, the martensite phase in the nugget zone may exhibit hardness within the range of 450 Hv to 475 Hv. The HAZ, characterized by a slower cooling rate, displays ferrite phase hardness levels below 350 Hv. Notably, resistance spot welding (RSW) cooling rates are generally sufficient for martensite formation in the nugget zone, as observed in previous studies [15]. Svensson et al. (2004) devised a method to estimate nugget region hardness by analyzing alloyed steel sheets with low carbon content, assuming complete martensitic transformation. Their findings revealed that spot welds in steels consist entirely of martensite, confirmed by comparing expected and measured hardness data [49]. In 2007, Kahraman studied microhardness distribution, noting that the welding nugget exhibited the highest hardness levels, followed by the HAZ, while the BM displayed comparatively lower hardness levels [50]. Pouranvari et al. 2020 demonstrated that the fusion zone has a significantly greater hardness than the base metal, attributed primarily to martensite formation within the fusion zone [51]. The welding process induces the formation of martensite and retained austenite in the nugget zone due to the melting stage and rapid cooling, contributing to increased hardness. The reduced hardness within the HAZ is linked to notable elastic distortion [15].

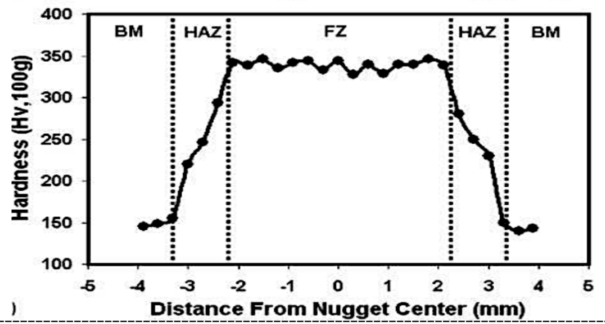

Fig. 6: Hardness profile. Adapted from [48].

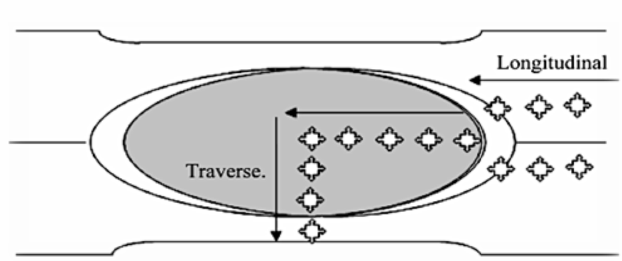

Fig. 7: Microhardness measurement. Adapted from [47].

5. Residual stresses

5.1. Residual stress in welding

In welding, residual stress results from mismatches between various components, various phases, or various regions within the same part brought on by non-uniform thermal strain, strain from solidification, and strains resulting from solid-state phase transformation [52]. During welding, the region around the weld pool invariably experiences residual tensile stresses in the welding direction, which are counterbalanced by compressive stresses farther from the weld line [53]. It is important to accurately quantify residual stress in welded fabrications, including repair welds [54]. The primary research focus on welding-induced residual stress has been the advancement of mathematical models and experimental methodologies aimed at predicting, quantifying, and mitigating residual stress across a range of joint geometries and welding conditions [55, 56]. The residual stresses in steel welds can be significantly influenced by transformation strains brought on by solid-state phase transformations, such as austenite to martensite or ferrite after cooling [57]. The residual stress distribution in weldment components is influenced by various factors, including the pre-existing residual stress during the manufacturing and fabrication processes, the properties of the materials of both the welded joint and the BM, the geometric properties of the interconnected constituents, the application of restraint during the welding process and the procedures to be followed during the operation after welding [58].

5.2. Types of residual stress in welding

The welding process induces residual stresses, encompassing both tensile and compressive forces within the welded component. This results in variable stress levels at different locations, particularly within the welded elements [59]. Shrinkage, quenching, and phase transformation are the primary factors contributing to residual stress in welding. Each of these stress-inducing mechanisms affects the distribution of residual stress differently, as illustrated in Figure 8. While compressive residual stress type is influenced by quenching and phase transformation, shrinking is responsible for the occurrence of tensile residual stress type [60]. The presence of tensile residual stress is typically harmful [61]. Tensile residual stress, commonly considered detrimental, can lead to issues such as stress-corrosion cracking, buckling deformation, and brittle fracture [62, 63]. On the other hand, the introduction of compressive residual stress can have favorable effects on welded components, enhancing fatigue strength, especially when present at the surface [61]. Residual tensile and compressive stresses coexist in welding components, but their distribution varies depending on the specific location. The improvement of a welding component can be achieved by applying targeted treatments based on the data related to residual stress distribution. Determining and understanding the welding residual stress distribution is crucial for enhancing component quality and mitigating negative impacts [61].

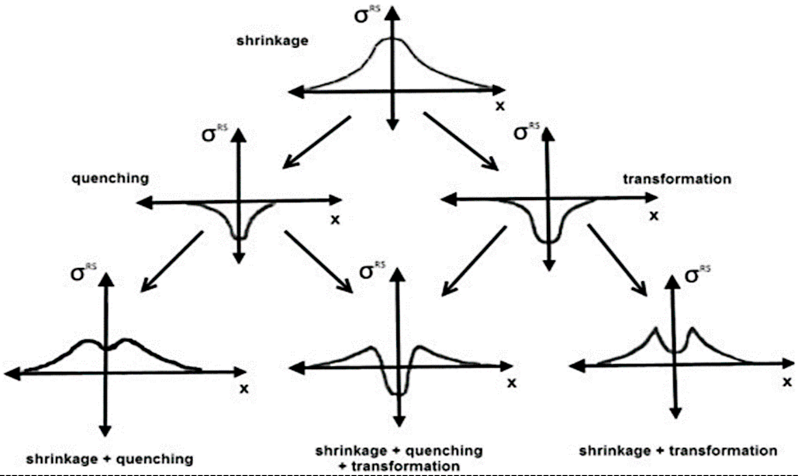

Fig. 8: Change of residual stress due to metallurgical processes during welding. Adapted from [64].

5.3. Residual stress in RSW

Residual stresses in RSW are more intricate than those found in other welding methods. These stresses arise from three main factors: rapid local heating and cooling, uneven plastic deformation, and changes in the material's microstructure during heating and cooling (phase transformation) [65]. Researchers have developed various methods to measure these stresses in spot welds, including measurements along the weld, on the surface, and at the center [66]. Around the center of the weld, the stresses are tensile (pulling apart) but transition to compressive (pushing together) as you move towards the edge. Similarly, the stresses perpendicular to the weld are compressive at the edge and tensile in the center [67, 68]. (Figure 9) shows a typical distribution of these stresses. Notably, the tensile stresses around the weld center are relatively uniform and equal to the material's yield strength. In contrast, the compressive stresses perpendicular to the weld are more concentrated, grow rapidly during cooling, and can trigger different types of cracking. The magnitude and distribution of these perpendicular stresses are significantly affected by the time the weld is held under pressure and the force applied by the electrodes [69].

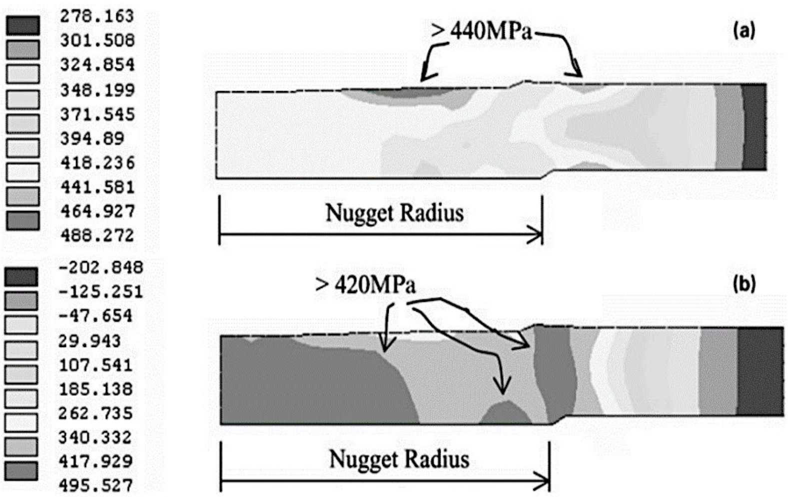

Fig. 9: The distributions of predicted residual stresses in HSLA steel (yield strength 450 MPa). (a) The residual stress acts in a radial direction. (b) The residual stress acts in a circumferential direction. Adapted from [62].

Welding heat and electrode force cause the molten material (fusion zone) to expand. This expansion creates compressive stresses in the surrounding cooler material. As the weld cools, shrinkage occurs, creating tensile stresses. Copper electrodes remove heat, affecting the cooling rate and stress levels. Moving towards the sheet edge reduces both tensile and compressive stresses inside and outside the weld zone [70]. The amount of residual stress in a spot weld depends mainly on the electrical current, weld time, and their interaction (Figure 10). Both higher currents and longer welding times reduce residual stress by increasing heat input [71]. Muhammed (2020) studied residual stress in spot-welded DP600 steel. Six out of seven samples welded with 7 kA current showed the highest stress, indicating higher hardness and strength compared to other samples. Increasing welding current generally increases compressive residual stress, suggesting a link between residual stress and mechanical properties [72]. Triyono et al (2010) used neutron diffraction to measure residual stresses at the interface of spot-welded carbon steel and austenitic steel. They found compressive residual stresses on both sides (carbon steel and stainless steel) in the normal, radial, and hoop directions, varying in magnitude with distance from the nugget center [73]. With an increasing current of the welding and time, the residual stresses increase, but the effect of the current is greater than the time [74]. Electrode force has little effect on this stress [75].

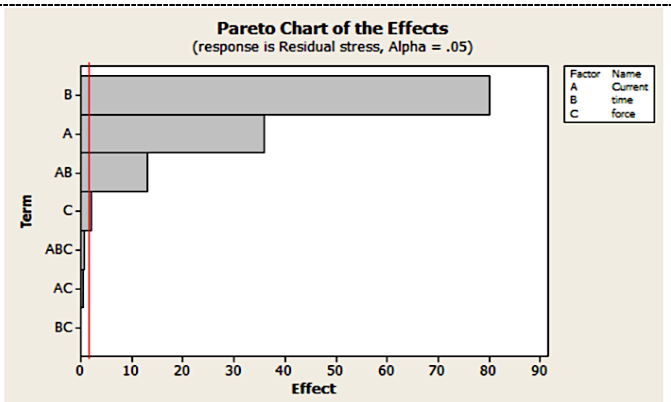

Fig. 10: The impact of spot weld parameters on the maximum residual stresses. Adapted from [72].

5.4. Measurement of stresses

The stresses can be determined for spot welds using non-destructive procedures of X-ray diffraction (XRD). Residual stresses can be calculated via XRD on a diametral cross-section. Measurements are taken either inside or on the spot's surface. There are macroscopic and microscopic residual stresses [66, 76]. Different types of residual stresses necessitate different measuring techniques. These stresses fall into three categories: macro, micro (intergranular), and atomic-scale. To achieve optimal results, the measurement technique should be tailored to the specific type of residual stress present [60].

5.4.1. X-ray diffraction method

Without damaging the material, X-ray diffraction (XRD) measures residual stresses on its surface (figure 11). XRD detects how applied or residual stress stretches or compresses the atomic planes within the metal's crystalline structure, causing elastic strains. By measuring these changes in spacing between atomic planes, XRD can indirectly determine the overall stress on the metal [77, 78]. The XRD technique is fast, reliable, safe for samples, and good at maintaining sample quality. However, when choosing a residual stress measurement technique, several factors should be considered, such as Specimen: For valuable, rare, or small specimens, a non-destructive technique is preferred. Machine/method feasibility: Techniques with less technology, easier handling, lower cost, and simpler analysis are preferable. Type and scale of residual stress: The chosen technique should be sensitive to the specific type and scale of residual stress present in the sample. In essence, the best residual stress measurement technique is the one that balances accuracy, cost, ease of use, and safety for the sample [79].

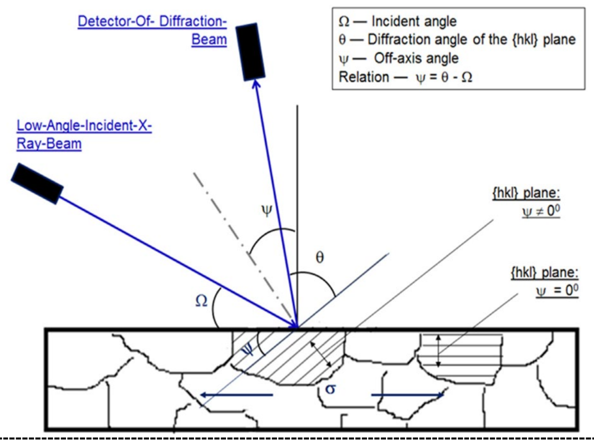

Fig. 11: X-ray diffraction method for measured residual stresses [80].

6. Effect of alloying elements on the alloy steel

Composed of a diverse mix of elements like silicon, boron, and nickel, alloy steel boasts enhanced properties like strength, hardness, and wear resistance table 1 show the effect of alloying element on alloy steel. The amount of these elements can range from 1% to 50%, impacting the categorization of alloy steel into two types: low and high. With 5% being the common dividing line, the presence of this threshold amount of alloying elements is often the defining characteristic of high-alloy steel [81]. The properties of the weld metal are influenced by both intentional and unintentional additions of alloying elements. These elements can be added through the filler material and flux, or they can be absorbed from the base metal during the welding process. Alloying elements serve two main purposes: 1) to achieve the desired strength level, and 2) to control the microstructure of the weld metal. However, the complex interactions between different elements make it difficult to predict the exact impact of any individual element on the final properties of the weld [82]. In complex commercial alloy steels, composed of several elements, the added components can exist in different forms: Free elements: Exist independently within the steel structure. Intermetallic compounds: Chemical bonds formed between iron and other alloying elements. Nonmetallic inclusions: Oxides, sulfides, or other non-metallic elements trapped within the steel. Carbides: Specific compounds formed between carbon and certain alloying elements. Dissolved solution: Alloying elements fully integrated within the iron matrix at an atomic level. The distribution of these elements falls into two categories: non-carbide forming elements: These elements, like nickel, silicon, cobalt, aluminum, copper, and nitrogen, do not form carbides with iron. Carbide-forming elements: These elements, including chromium, manganese, molybdenum, tungsten, vanadium, titanium, zirconium, and niobium, readily form stable carbides in the steel [83]. Metal elements can be added to steel to form stable carbides. This can be done by adding chemical compounds that contain both carbon and iron or by incorporating them directly into the solid solution. The way these elements are distributed depends on how much carbon is in the steel and whether there are other elements present that can also form carbides. Steels that have these carbide-forming elements show two separate peaks in the rate at which austenite decomposes. These peaks are separated by a period where the austenite is relatively stable, as shown in (Figure 12).[84].

Table 1: Affect some alloying elements on properties of alloy steel [86]

Alloying Element	Properties of alloy steel
Cr	Increase hardenability, high-temperature strength, Abrasion Resistance, and Corrosion Resistance
Ti	High Temperature Strength, Hardenability.
Ni	Corrosion Resistance, Hardenability, Ductility and Toughness,
W	Hardenability, High Temperatures Strength, Abrasion Resistance, Abrasion Resistance.
V	Hardenability, High Temperature Strength, Abrasion Resistance,
Mo	Corrosion Resistance, Abrasion Resistance, Hardenability.

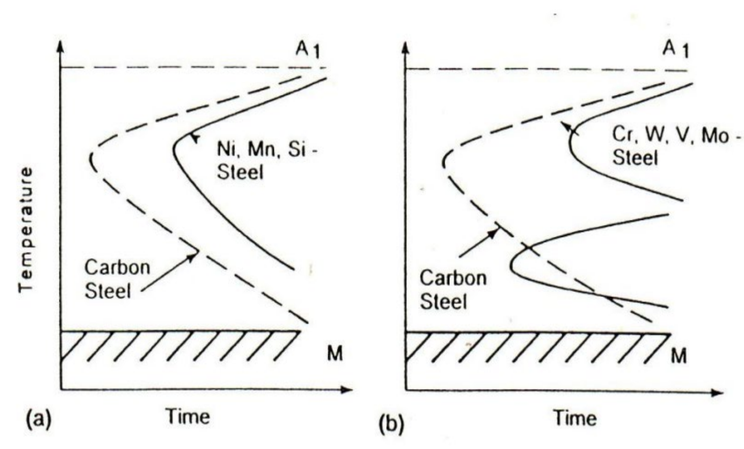

Fig. 12: Displays diagrams depicting isothermal transformation. (a) Carbon steel and steel alloyed with non-carbide-forming elements are two types of steel compositions. (b) Carbon steel and steel alloyed with the carbide-forming element are two distinct categories of steel compositions. Adapted from [84].

The hardness of ferrite is influenced by the presence of alloying elements that form solid solutions. Figure 13 illustrates the observed increase in hardness resulting from the introduction of a substitutional solution. Si and Mn are commonly found alloying elements that significantly impact ferrite's hardness. In contrast, Cr has the least pronounced effect on hardness increase. Due to this rationale, Cr is an exceptionally advantageous alloying element in steel intended for cold working processes that necessitate superior hardenability [85].

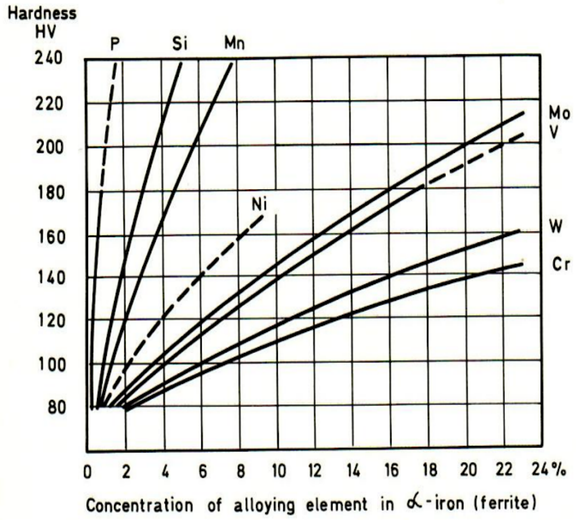

Fig. 13: Illustrates the impact of substitutional alloying element additions on the hardness of ferrite, as reported in reference. Adapted from [85].

7. Conclusion

The following points can be concluded for the current review:

1. RSW is a key assembly procedure in the automotive and aviation industries due to its efficiency and speed.
2. As the weld current and time increase, the size of the weld nugget also increases. This results in increased values of tensile-shearing strength.
3. The reason for the formation of residual stresses in welded parts is rapid cooling and phase transformation.
4. In the weld center are tensile residual stresses that transform into a compressive state as they approach the edge of the weld nugget.
5. The presence and incorporation of an alloying element in LAS significantly impact the microstructure, consequently influencing the mechanical properties.

Acknowledgement

First of all, profusely all thanks are to ALLAH Lord of all creation who enables me to achieve this work. I would also like to express my deepest appreciation to my supervisors, Asst. Prof. Dr. Muhaed Sadiq Jafar. & Prof. Dr. Sabah.M. Thahab for their valuable efforts, support, and advice throughout this research. Deep thanks and gratitude to my father who was missed now for him. Finally, words are not enough to dedicate thanks to "My mother", "My brothers", "My sister" and "Friends" and "Colleagues" who have never forgotten me during a hard time.

References

[1] Callister, W.D. and D.G. Rethwisch, Fundamentals of materials science and engineering. Vol. 471660817. 2000: Wiley London.
[2] Callister, W., et al., Properties of Selected Engineering Materials (Appendix B). 2007: p. A3-A30.
[3] Colegrove, P., et al., Welding process impact on residual stress and distortion. 2009. 14(8): p. 717-725.
[4] Balasingh, C., A.J.M.m. Singh, and Processes, Residual Stresses and Their Measurements by X-ray Difraction Methods. 2000. 12(2/3): p. 269-280.
[5] Ferro, P., et al., The influence of phase transformations on residual stresses induced by the welding process—3D and 2D numerical models. 2006. 14(2): p. 117.
[6] Chabok, A., et al., Effect of pulse scheme on the microstructural evolution, residual stress state and mechanical performance of resistance spot welded DP1000-GI steel. 2018. 23(8): p. 649-658.
[7] Luo, Y., et al., Study on the thermo-effect of nugget growing in single-phase AC resistance spot welding based on the calculation of dynamic resistance. 2016. 78: p. 18-28.
[8] Moshayedi, H. and I.J.J.o.M.P.T. Sattari-Far, Resistance spot welding and the effects of welding time and current on residual stresses. 2014. 214(11): p. 2545-2552.
[9] Sedighi, M., D. Afshari, and F.J.P.o.t. I.o.M.E. Nazari, Part C: Journal of Mechanical Engineering Science, Investigation of the effect of sheet thickness on residual stresses in resistance spot welding of aluminum sheets. 2018. 232(4): p. 621-638.
[10] Avazkonandeh-Gharavol, M., et al., Effect of copper content on the microstructure and mechanical properties of multipass MMA, low alloy steel weld metal deposits. 2009. 30(6): p. 1902-1912.
[11] Thornton, M., et al., Progress in NDT of resistance spot welding of aluminum using ultrasonic C-scan. 2012. 48: p. 30-38.
[12] Hwang, I.S., M.J. Kang, and D.C.J.P.E. Kim, Expulsion reduction in resistance spot welding by controlling of welding current waveform. 2011. 10: p. 2775-2781.
[13] Podržaj, P., et al., Overview of resistance spot welding control. 2008. 13(3): p. 215-224.

[14] Özyürek, D.J.M. and design, An effect of weld current and weld atmosphere on the resistance spot weldability of 304L austenitic stainless steel. 2008. 29(3): p. 597-603.
[15] Bharaj, A.S., et al., Study of resistant spot welding and its effect on the metallurgical and mechanical properties _ a review. 2023.
[16] Arumugam, A., N.J.J.o.M.S. Charde, and E. A, A mechanical study of spot weld growth in mild steel, 302 austenitic stainless steel and both materials joined. 2011. 1(2A): p. 243.
[17] Zhao, D., et al., Multi-objective optimization of the resistance spot welding process using a hybrid approach. 2021. 32(8): p. 2219-2234.
[18] Darwish, S. and S.J.J.o.M.P.T. Al-Dekhial, Micro-hardness of spot welded (BS 1050) commercial aluminum as correlated with welding variables and strength attributes. 1999. 91(1-3): p. 43-51.
[19] Shamsul, J., M. Hisyam, and T.J.J.o.A.S.R. Muhibbah, Study of spot welding of austenitic stainless steel type 304. 2007. 3(11): p. 1494-1499.
[20] Zhang, H. and J.J.E.a.o.p. Senkara, Resistance welding: fundamentals and applications, 2006
[21] Raut, M., V.J.I.J.o. M.E. Achwal, and R. Research, Optimization of spot welding process parameters for maximum tensile strength. 2014. 3(4): p. 507-517.
[22] Eisazadeh, H., et al., New parametric study of nugget size in resistance spot welding process using finite element method. 2010. 31(1): p. 149-157.
[23] Muhammad Safwan, M.M., Investigation on the mechanical properties and microstructure analysis of micro-resistance spot welding between stainless steel 316L and Tl-6AL-4V/Muhammad Safwan Mohd Mansor. 2020, University Malaya.
[24] Oba, P.N., QUALITY ANALYSIS MODELLING FOR DEVELOPMENT OF A PROCESS CONTROLLER IN RESISTANCE SPOT WELDING USING NEURAL NETWORKS TECHNIQUES. 2006.
[25] Afshari, D., et al., An approach in prediction of failure in resistance spot welded aluminum 6061-T6 under quasi-static tensile test. 2012. 226(6): p. 1026-1032.
[26] Alali, M. and M.G. Alnaffakh, Characterization of AISI 316L Stainless Steel/Low Alloy Steel Resistance Spot Dissimilar Weld. Metallography, Microstructure, and Analysis, 2023: p. 1-12.
[27] Manladan, S.M., et al., A review on resistance spot welding of aluminum alloys. 2017. 90: p. 605-634.
[28] Zhao, D., et al., Effects of electrode force on microstructure and mechanical behavior of the resistance spot welded DP600 joint. 2013. 50: pp. 72-77.
[29] Liu, T., et al. Microstructure of resistance spot weld ultra high strength steel Q&P980. in IOP Conference Series: Materials Science and Engineering. 2019. IOP Publishing.
[30] Sun, X., E.V. Stephens, and M.A.J.W.J.-N.Y.-. Khaleel, Effects of fusion zone size and failure mode on peak load and energy absorption of advanced high-strength steel spot welds. 2007. 86(1): p. 18.
[31] Liao, X., et al., Microstructures in a resistance spot welded high strength dual phase steel. 2010. 61(3): p. 341-346.
[32] Lu, Y., Resistance, and Ultrasonic Spot Welding of Light-Weight Metals. 2018: The Ohio State University.
[33] Liu, X., et al., Mechanical properties in double pulse resistance spot welding of Q&P 980 steel. 2019. 263: p. 186-197.
[34] Alimohamady, A., et al., Friction stir welding of EN 10130 low carbon steel. 2020. 38(3): p. 269-277.
[35] Razmpoosh, M., et al., The microstructural evolution and mechanical properties of resistance spot welded Fe–31Mn–3Al–3Si TWIP steel. 2015. 67: p. 571-576.
[36] Al-Mukhtar, A. Review of resistance spot welding sheets: processes and failure mode. in Advanced Engineering Forum. 2016. Trans Tech Publ.
[37] Annan, K.A., et al., Resistance spot welding of a thin 0.7 mm EN10130: DC04 material onto a thicker 2.4 mm 817M40 engineering steel. 2021. 121(10): p. 549-556.
[38] Al-Mukhtar, A.J.B.U., Spot Welding Efficiency and Its Effect on Structural Strength of Gas Generator and Its Performance. 2002.
[39] Aslanlar, S.J.M. and Design, The effect of nucleus size on mechanical properties in electrical resistance spot welding of sheets used in the automotive industry. 2006. 27(2): p. 125-131.
[40] Pouranvari, M., S.J.M.S. Marashi, and Technology, Factors affecting mechanical properties of resistance spot welds. 2010. 26(9): p. 1137-1144.
[41] Pouranvari, M.J.I.J.o. M.S. and Engineering, Effect of welding current on the mechanical response of resistance spot welds of unequal thickness steel sheets in tensile-shear loading condition. 2011. 2(6): p. 178-189.
[42] Jaber, H., et al., Dissimilar spot welding of dual phase steel/ferritic stainless steel: phase transformations. 2014. 19(7): p. 565-571.
[43] Pouranvari, M. and S.J.W.J. Marashi, Failure mode transition in AISI 304 resistance spot welds. 2012. 91(11): p. 303-309.
[44] Pouranvari, M.J.M.S. and E. A, Susceptibility to interfacial failure mode in similar and dissimilar resistance spot welds of DP600 dual phase steel and low carbon steel during cross-tension and tensile-shear loading conditions. 2012. 546: p. 129-138.
[45] Pouranvari, M., S.J.I. Marashi, and Steelmaking, Failure of resistance spot welds: tensile shear versus coach peel loading conditions. 2012. 39(2): p. 104-111.
[46] Khodabakhshi, F., et al., Mechanical properties and microstructure of resistance spot welded severely deformed low carbon steel. 2011. 529: p. 237-245.
[47] Al-Mukhtar, A. and Q.J.M.S.A. Doos, Cracking phenomenon in spot welded joints of austenitic stainless steel. 2013. 4: p. 656-662.
[48] Pouranvari, M., S.J.M.S. Marashi, and Technology, Similar and dissimilar RSW of low carbon and austenitic stainless steels: effect of weld microstructure and hardness profile on failure mode. 2009. 25(12): p. 1411-1416.
[49] Svensson, L.J.W.i.t.W., Prediction of the hardness of spot welds in steels. 2004. 48(11-12): p. 31-35.
[50] Kahraman, N.J.M. and design, The influence of welding parameters on the joint strength of resistance spot-welded titanium sheets. 2007. 28(2): p. 420-427.
[51] Pouranvari, M. and P.J.A.M.R. Marashi, Resistance spot welding of unequal thickness low carbon steel sheets. 2010. 83: p. 1205-1211.
[52] Withers, P.J., H.J.M.s. Bhadeshia, and Technology, Residual stress. Part 1–measurement techniques. 2001. 17(4): p. 355-365.
[53] De, A., et al., A perspective on residual stresses in welding. 2011. 16(3): p. 204-208.
[54] Dong, P., et al., Analysis of residual stresses at weld repairs. 2005. 82(4): p. 258-269.
[55] Boulton, N. and H.L.J.P.o.t.I.o.M.E. Martin, Residual stresses in arc-welded plates. 1936. 133(1): p. 295-347.
[56] Shim, Y., et al., Determination of residual stresses in thick-section weldments. 1992. 71(9): p. 305-312.
[57] Andersson, B., Thermal stresses in a submerged-arc welded joint considering phase transformations. 1978.

[58] Karlsson, R. and B. Josefson, Three-dimensional finite element analysis of temperatures and stresses in a single-pass butt-welded pipe. 1990.
[59] Ju, J.-B., et al., Determination of welding residual stress distribution in API X65 pipeline using a modified magnetic Barkhausen noise method. 2003. 80(9): p. 641-646.
[60] Assis, J., et al., X-ray analysis of residual stress distribution in the weld region. 2002. 45: p. 225-31.
[61] Nasir, N.S.M., et al., Review on welding residual stress. 2006. 2(5): p. 8-10.
[62] Webster, G. and A.J.I.J.o.F. Ezeilo, Residual stress distributions and their influence on fatigue lifetimes. 2001. 23: p. 375-383.
[63] Dong, P.J.S., T.o. Welding, and Joining, Residual stresses and distortions in welded structures: a perspective for engineering applications. 2005. 10(4): p. 389-398.
[64] Macherauch, E. Origin, measurement, and evaluation of residual stresses. Residual stresses in science and technology. in Papers presented at the Int. Conf. on residual stresses, 1986 Garmisch-Partenkirchen. 1987.
[65] Khanna, S., et al., Residual stresses in resistance spot welded steel joints. 2008. 13(3): p. 278-288.
[66] Anastassiou, M., et al., Residual stresses and microstructure distribution in spot-welded steel sheets: relation with fatigue behavior. 1990. 125(2): p. 141-156.
[67] Nodeh, I.R., S. Serajzadeh, and A.H.J.J.o.m.p.t. Kokabi, Simulation of welding residual stresses in resistance spot welding, FE modeling and X-ray verification. 2008. 205(1-3): p. 60-69.
[68] Afshari, D., et al., On residual stresses in resistance spot-welded aluminum alloy 6061-T6: experimental and numerical analysis. 2013. 22: p. 3612-3619.
[69] Sun, X., and P.J.W.J.-N.Y.-. Dong, Analysis of aluminum resistance spot welding processes using coupled finite element procedures. 2000. 79(8): p. 215-S.
[70] Afshari, D., et al., Residual stresses in resistance spot welded AZ61 Mg alloy. 2019. 118(2): p. 275-290.
[71] Cha, B. and S.-J.J.J.o.M.S. Na, A study on the relationship between welding conditions and residual stress of resistance spot welded 304-type stainless steels. 2003. 22(3): p. 181-189.
[72] Elitas, M. and B.J.M.T. Demir, Residual stress evaluation during RSW of DP600 sheet steel. 2020. 62(9): p. 888-890.
[73] Triyono, T., et al., Residual stress measurements at the interface of spot welded dissimilar metals between carbon steel and austenitic stainless steel. 2010. 7(2): p. 319-324.
[74] Moshayedi, H., & Sattari-Far, I. (2014). Resistance spot welding and the effects of welding time and current on residual stresses. Journal of Materials Processing Technology, 214(11), 2545-2552.
[75] Afshari, D., Mechanical properties of resistance spot welds in lightweight applications. 2013, KTH Royal Institute of Technology.
[76] Shinozaki, M., et al., Improvement in fatigue strength of spot welded high strength sheet steel joints. 1982. 68(9): p. 1444-1451.
[77] Norton, J. and D.J.P.o.t.s.f.e.s.a. Rosenthal, Stress measurement by x-ray diffraction. 1944. 1(2): p. 73-76.
[78] Norton, J. and D.J.P.o.t.s.f.e.s.a. Rosenthal, Application of the x-ray method of stress measurement to problems involving residual stress in metals. 1944. 1(2): p. 81-90.
[79] Macherauch, E.J.A.i.s.t., Introduction to residual stress. 2014. 4: p. 1-36.
[80] Luo, Q., & Yang, S. Uncertainty of the X-ray diffraction (XRD) sin2 ψ technique in measuring residual stresses of physical vapor deposition (PVD) hard coatings. Coatings, 2017.7(8), 128.
[81] Papavinasam, S., Corrosion control in the oil and gas industry. 2013: Elsevier.
[82] Grong, O. and D.K.J.I.m.r. Matlock, Microstructural development in mild and low-alloy steel weld metals. 1986. 31(1): p. 27-48.
[83] Totten, G.E. and M.A.J.S.h.t.h. Howes, Distortion of heat-treated components. 1997: p. 251-292.
[84] Maalekian, M., Early Stages of Precipitation. 2007.
[85] THELNING, K.J.B., Mackays of Great Britain: Chatham Ltd, Steels And Its Heat Treatment, 2aed. 1984.
[86] Ibrahim, M., Zakaria, Z., Mustapha, A. A., Surin, D. D, et al. Sensors & Transducers.Magnetic flux leakage (MFL) capsule material selection and its robustness analysis in oil and gas pipeline. 2013. 156(9), 67.